HHS Public Access

Author manuscript

Schizophr Res. Author manuscript; available in PMC 2019 June 20.

Published in final edited form as:

Schizophr Res. 2018 July ; 197: 209–218. doi:10.1016/j.schres.2017.12.004.

Substantia nigra ultrastructural pathology in schizophrenia

Courtney K. Walker[a], **Joy K. Roche**[a], **Vidushi Sinha**[a], **Rosalinda C. Roberts**[b]

[a]Department of Psychology, University of Alabama at Birmingham

[b]Department of Psychiatry and Behavioral Neurobiology, University of Alabama at Birmingham

Abstract

Schizophrenia is a severe mental illness affecting approximately 1% of the population worldwide. Despite its prevalence, the cause remains unknown, and treatment is not effective in all patients. Dopamine is thought to play a role in schizophrenia pathology, yet the substantia nigra (SN), the origin of dopaminergic pathways, has not been studied extensively in schizophrenia. In this study, electron microscopy was used to examine neurons, oligodendrocytes, and myelinated axons in the SN of normal controls (NCs, n=9) and schizophrenia subjects with varying response to antipsychotic drugs [SZ, n=14; treatment resistant (TR) = 6, treatment responsive (RESP) = 6, unknown = 2]. Postmortem tissue was analyzed for qualitative and quantitative markers of ultrastuctural integrity. A significantly higher percentage of axons in the schizophrenia group had inclusions in the myelin sheath compared to NCs (SZ: 3.9±1.7, NC: 2.6±2.0). When considering treatment response, a significantly higher percentage of axons lacked cytoplasm (TR: 9.7±5.5, NC: 3.5±2.3), contained cellular debris (TR: 7.5±3.2, NC: 2.3±1.3) or had protrusions in the myelin sheath (TR: 0.4±0.5, NC: 0.2±0.3). The G-ratio, a measure of myelin thickness, was significantly different between treatment response groups and was greater in TR (0.72±0.02) as compared to NCs (0.68±0.03), indicating decreased myelination in TR. These findings, which suggest myelin pathology in the SN in schizophrenia, are consistent with findings elsewhere in the brain. In addition, our results suggest cytoskeletal abnormalities, which may or may not be associated with myelin pathology.

Keywords

mitochondria; myelin; axons; treatment resistance; postmortem

Corresponding author information: Rosalinda Roberts, Sparks Center 865, 1720 2nd Avenue South, Birmingham, AL 35294, Tel. 205-996-9373, Fax 205-996-9377, rcusidor@uab.edu.

Contributors

CKW wrote the first draft of the manuscript and edited it, performed the vast majority of data collection and analysis. JKR prepared and sectioned all of the tissue for electron microscopy. VS analyzed the data on oligodendrocytes. RCR designed the experiment and protocol, supervised the other authors and edited the final manuscript.

Conflict of interest

The authors have nothing to disclose.

1. Introduction

Schizophrenia (SZ), a severe mental illness affecting approximately 1% of the population, is characterized by positive, negative, and cognitive symptoms (American Psychiatric Association, 2013). Antipsychotic drugs (APDs), used to treat SZ (see as review Seeman, 2002), function by blocking striatal dopamine D_2 receptors (Carlsson and Lindqvist, 1963; Creese et al., 1977). The substantia nigra (SN) and ventral tegmental area are the major origin of dopaminergic pathways (Fallon et al., 1978a,b; Gaspar et al., 1992). While many studies have examined targets of the SN in SZ, far fewer studies have examined the SN itself, and these have often reported conflicting results.

Imaging studies have shown that more dopamine is produced in the SN in SZ (Watanabe et al., 2014), there is evidence of higher glutamate levels (White et al., 2015), and the SN is hyperactive, which is linked with both prefrontal cortex hypofunction and striatal hyperfunction (Yoon et al., 2013, 2014). Some postmortem studies show complementary evidence, such as increased levels of tyrosine hydroxylase (TH) mRNA or protein, indicating elevated dopamine synthesis capacity (Mueller et al., 2004; Toru et al., 1988; Howes et al., 2013; Schoonover et al., 2016). However, some have found no difference (Ichinose et al., 1994) or decreased levels of TH protein in rostral SN (Perez-Costas et al., 2012). The deficit of TH protein rostrally was due to decreased TH translation, rather than transcription (Perez-Costas et al., 2012) or neuronal loss (Rice et al., 2016). Additionally, abnormal expression of key cytochrome c oxidase subunits was seen in the SN in SZ (Rice et al., 2014), suggesting metabolic abnormalities.

Abnormalities in oligodendrocytes and myelinated axons have been observed at imaging, genetic, and ultrastructural levels. Decreased white matter volume has been seen in SZ (Bora et al., 2011; De Peri et al., 2012; Di et al., 2009; Haijma et al., 2013; Kubicki et al., 2007; Kuswanto et al., 2012; Olabi et al., 2011; Samartzis et al., 2014; Yao et al., 2013), suggesting oligodendrocyte and myelin pathology. Several genes associated with oligodendrocyte function and the myelin sheath are downregulated in SZ, altering their development and function (Xiao et al., 2008). Ultrastructural studies have shown oligodendrocyte pathologies, including swollen appearance, chromatin condensation, and membranous myelin-like inclusions, as well as altered myelin thickness and a greater percentage of pathologically myelinated fibers in prefrontal cortex (Uranova et al., 2011; Vikhreva et al., 2016).

Despite the prevalence of SZ, few advances have been made in the refinement of APDs. Generally, APDs alleviate positive symptoms with little to no effect on negative symptoms and cognitive impairment (McEvoy, 2006). Furthermore, treatment response is not uniform among patients. One-fifth to one-third of patients do not respond to APDs, while the remainder show varying levels of recovery (Conley and Kelly, 2001). Although what causes these differences in response is unknown, there is evidence of a biological basis (Altamura et al., 2005; Arango et al., 2003; Beerpoot et al., 1996; Roberts et al., 2012; Sheitman and Lieberman, 1998; Somerville et al., 2011).

The goal of this study was to determine whether there are structural differences in the SN that are associated with SZ pathology and treatment response. Electron microscopy of postmortem human tissue was used to analyze neurons, oligodendrocytes, and myelinated axons. Because animal models of SZ do not perfectly replicate the disease, postmortem studies such as this one are valuable in SZ research.

2. Methods

2.1 Tissue Samples and Preparation

Postmortem human brain tissue was obtained from the Maryland and Alabama Brain Collections from 9 controls and 14 schizophrenia subjects with permission of next of kin. Cases were diagnosed by two psychiatrists' independent evaluations, as described previously (McCollum et al., 2015). Diagnosis of treatment response or resistance was conducted as detailed by Roberts et al. (2009, 2012). Briefly, treatment response or resistance was diagnosed based on established criteria (Conley and Kelly, 2001; Kane (1988): (1) no clinical improvement during two prior drug treatment periods; (2) at least five years with no period of good social or occupational functioning; and (3) presence of persistent positive psychotic symptoms throughout the person's life. If all were present, a diagnosis of treatment resistance was made. Control and schizophrenia subjects were matched for age, race, gender, pH, and postmortem interval, as shown in Table 1.

The midbrains, containing the SN, were immersed in a cold solution (4°C) of 4% paraformaldehyde and 1% glutaraldehyde in 0.1 M phosphate buffer (PB). For most of the cases used in the present study, the dorsal striatum (see for examples Roberts et al., 2009, 2012; Somerville et al., 2011a,b), nucleus accumbens (McCollum et al., 2015), and prefrontal cortex (see for example Roberts et al., 2005) have been previously analyzed for synaptic organization. The tissue was stored at 4°C in fixative until used. The SN was blocked in the transverse plane at the level of the 3rd nerve rootlets and red nucleus. Six series of 40 μm sections were cut using a Vibratome (HM 650V microtome, Thermo Scientific).

2.2 Electron Microscopy

Samples were flat-embedded for electron microscopy using standard techniques, described by McCollum and Roberts (2014). Briefly, the sections were rinsed twice in PB for 5 minutes each, immersed in 1% osmium tetroxide in 0.1 M PB at room temperature in the dark for 1 hour, rinsed four times for 5 minutes each in PB, then dehydrated at room temperature in the dark in 50% and then 70% EtOH. The tissue was stained en bloc in a 1% uranyl acetate solution in 70% EtOH for 1 hour for contrast, and then rinsed in 70% EtOH two times for 5 minutes each. The tissue was dehydrated in increasing concentrations of EtOH, followed by 100% propylene oxide, then embedded in epon resins, and heated at 60°C for 72 hours.

For each case, blocks at least 240 μm apart rostrocaudally, were used to obtain semithin sections. The location of these blocks was in the dorsal tier of the substantia nigra pars compacta in the middle of the mediolateral SN. These sections (250 nm thickness) were

collected using an ultramicrotome (Leica EM UC6), mounted on glass slides, stained with Toluidine Blue and cover slipped for reference. These sections were used to verify that the block face contained dopaminergic neurons (identified by size and neuromelanin pigment). Serial thin sections (90 nm thickness) were collected, mounted on Formvar-coated copper grids, and photographed at 80KV on a Hitachi 87650 transmission electron microscope using a Hamamatsu ORCA-HR digital camera.

Micrographs were taken at the following magnifications: neurons, 5,000×; myelinated axons and oligodendrocytes, 10,000×; and neuronal rough endoplasmic reticulum (rER), 25,000×. A total of 230 neurons, 313 oligodendrocytes, and 5,336 myelinated axons were photographed and analyzed. On average, 26 micrographs of rER were photographed per case. Authors were blinded to case diagnosis throughout microscopy and data collection.

2.3 Data Collection

2.3.1 Neurons and rER—At least ten dopamine neurons, identified by morphological criteria, were photographed and analyzed per case. Dopaminergic neurons were identified by their large cell bodies that usually contained neuromelanin granules and numerous stacks of rER as defined by Domesick et al., (1983) (Figure 1A,B). Neurons too large to fit in one micrograph were stitched together using PanaVue ImageAssembler3. Data were obtained from single thin sections. Mitochondria (n=13,458) in the somata were numbered in Adobe Photoshop C4 and diameters were measured along the short axis using ImageJ. The number of mitochondria per square micron of cytoplasm was calculated using ImageJ.

Cells contained variable amounts of rER. If a neuron contained similar rER throughout, approximately 3 micrographs were taken. In those containing clusters with notably different organization, micrographs were taken of the different clusters to ensure the overall rER organization was well-represented. rER organization was assessed using a rating scale, that ranged from 1–4: 1, highly disorganized and mostly scattered ribosomes; 2, a few strands; 3, at least 3 parallel strands; and 4, four or more perfectly organized strands (Figure 1C–F). Averages of rER organization ratings were calculated per case.

2.3.2 Oligodendrocytes—At least 10 oligodendrocytes, identified by morphological criteria, were photographed per case. Oligodendrocytes were identified by a round or oval-shaped nucleus with heterochromatin on the nuclear border (Uranova et al., 2001), light to medium density cytoplasm and defined cellular borders (Figure 2). Areas of oligodendrocyte soma, nuclei, heterochromatin, and euchromatin were measured, and the percent area of the nucleus composed of heterochromatin or euchromatin was calculated. The presence of amorphous inclusions, myelin inclusions, and filamentous cellular inclusions was noted, and the proportion of oligodendrocytes with each characteristic was calculated. Additionally, a rating scale was used to assess cytoplasmic integrity that ranged from 1–5, with 1 having the least integrity (little to no cytoplasm) and 5 indicating best integrity (full, even cytoplasm and few inclusions) (Figure 2).

2.3.3 Myelinated Axons—At least ten random fields of myelinated axons were photographed per case. The G-ratio, the ratio of axonal diameter to total (axon+myelin) diameter, was used to measure the degree of myelination. This value accounts for variability

in axonal size, and allows for comparison amongst axons. Axonal and total diameters were measured along the short axis. Myelin thickness and the G-ratio were calculated (Figure 3). Mitochondria (n=1,489) in numbered axons were counted and measured, as described in 2.3.1.

An average of 160 axons per case (n=3,669) were assessed for: normal axon; lack of cytoplasm; condensed, hyperdark, displaced, and/or disorganized contents; vacuolization; cellular debris; and myelin inclusions. The myelin sheath was assessed for being normal, unraveled, hypodense, having redundant parts, or containing inclusions. Unraveled sheaths were subdivided into two groups: <50% unraveled and ≥50% unraveled. Redundant myelin was rated as a protrusion or a tail. Qualitative assessments were expressed as the percent of axons with a given characteristic (Figure 4); although most of the examples are from SZ, these pathologies are found in NC as well.

2.4 Statistical Analysis

Demographics and tissue quality were tested using ANOVA and/or t-tests. Categorical variables were assessed using a chi-square test. Two comparisons were made in this study: 1) NC vs SZ and 2) NC vs RESP vs TR. Data was tested for normality with a Kolmogorov-Smirnov test. For two-group comparisons, parametric measures were assessed for significance using a t-test, while nonparametric measures were assessed with a Mann-Whitney U-test. For three-group comparisons, parametric measures were assessed for significance using ANOVA, while Kruskal-Wallis H test was used for nonparametric data. Significant omnibus tests were followed by planned, uncorrected comparisons: parametric tests were followed by an uncorrected Fisher's LSD test, while nonparametric tests were followed by an uncorrected Dunn's comparison.

3. Results

3.1 Case Demographics

NC and SZ groups did not differ significantly in age, race, sex, pH, or postmortem interval (Table 1). Treatment response groups were also well-matched for these demographics and age of onset and duration of illness. There was a difference between RESP and TR in type of APD, atypical (A) or typical (T), taken ($p<0.007$; RESP: 4A, 0T; TR: 2A, 4T, 2OFF).

3.2 Neurons

No differences were detected between NC and SZ for mitochondrial diameter, number of mitochondria per μm^2 of cytoplasm, rER rating, or percentage of each rating (Figure 5). There were also no differences observed in these measures between treatment response groups.

3.3 Oligodendrocytes

No significant differences were detected between NC and SZ for areas of oligodendrocyte somata, nuclei, heterochromatin and euchromatin, or percent of the nucleus containing heterochromatin or euchromatin. Additionally, these groups showed similar proportions of oligodendrocytes with amorphous inclusions, myelin inclusions, and filamentous cellular

inclusions. The average cytoplasmic integrity rating and percentage of each was not significantly different between groups. There were no significant differences found between treatment response groups for oligodendrocyte measurements (Figure 6).

3.4 Myelinated Axons

3.4.1 NC vs SZ—SZ subjects had a greater percentage of axons with inclusions in the myelin sheath than NCs ($p<0.039$, SZ: 3.90±1.72, NC: 2.63±2.00). No significant differences were detected in total diameter, axon diameter, myelin thickness, G-ratio or mitochondrial diameter. There were also no significant differences found between groups in percentages of axons whose cytoplasm was normal, condensed, hyperdark, displaced, vacuolized, disorganized, absent, contained cellular debris, or contained myelin inclusions. Finally, no differences were observed between groups for percentages of myelin sheaths that were normal, unraveled, hypodense, or redundant. Results are shown in Figure 7.

3.4.2 NC vs RESP vs TR—The G ratio was significantly different among treatment response groups ($p<0.046$) with a greater G-ratio in TR (0.72±0.02) than NC (0.68±0.03). The percentage of axons lacking cytoplasm also differed among treatment response groups ($p<0.039$); specifically, TR (9.70±5.48) had more axons lacking cytoplasm than NC (3.47±2.28). Additionally, there was a difference ($p<0.01$) in the percentage of axons containing cellular debris. TR (7.45±3.16) had more axons containing cellular debris than NC (2.35±1.28). No significant difference was detected between treatment response groups for the remaining measurements listed in 3.4.1. Results are shown in Figure 7.

4. Discussion

In SZ, more axons had inclusions in the myelin sheath. Axons in TR appeared less healthy than those of NC, as indicated by axons having larger G-ratios and more axons lacking cytoplasm, containing cellular debris, or having a protrusion in the myelin sheath. No differences in structural integrity were detected in neurons and oligodendrocytes in the SZ group as a whole or divided by treatment response.

4.1 Limitations

4.1.1 Sample size—One limitation of this study is the small sample size, common to ultrastructural studies of postmortem human brain tissue due to limited availability of suitable tissue. Studies of this type are especially valuable for illnesses like schizophrenia that cannot be fully modeled in animals. Despite this limitation, our findings of altered G-ratio and increased myelin pathology are similar to observations in an ultrastructural study of prefrontal cortex in another cohort of schizophrenia subjects (Uranova et al., 2011).

4.1.2 Antipsychotic drug use—APD effects should be considered as a potential confound when interpreting data between NC and SZ. APDs can facilitate activation and proliferation of oligodendrocyte progenitor cells (Niu et al., 2010; Wang et al., 2010) and increase expression of oligodendrocyte transcription factors 1 and 2 (Olig 1 and Olig 2) (Fang et al., 2013). In the present study, SZ had more axons with inclusions in the myelin

sheath; however, APDs generally promote myelination, so it is unlikely that APDs are responsible for this difference.

There was a difference in type of APD taken between RESP (2A, 4T) and TR (4A, 2OFF). However, APDs only alleviate positive symptoms and, aside from clozapine, both types do so to the same extent (Kane et al., 1988; Meltzer, 1997; Lieberman et al., 2005; McEvoy, 2006). Although the SZ subgroups had different numbers of subjects on typical versus atypical APDs, it seems unlikely that the difference in results between subgroups is related to medication. Haloperidol can cause shrinkage of TH-immunostained neurons in rat SN (Marchese et al., 2002); however, neuronal size was not considered in the present study. Studies have provided evidence that atypical APDs increase myelin production (Bartzokis et al., 2009; Thomas, 2006). In our study, axons from RESP did not have more myelin, but had less, as indicated by the greater G-ratio. This is the opposite of what would be expected if our finding was due to APD effects, suggesting medication status did not affect our findings.

4.2 Distribution of rER ratings

Most rER was categorized as having a few scattered strands, and appeared more disorganized than organized. It was expected that most rER in normal cells would be highly organized; rER plays an important role in protein synthesis, and abnormalities in rER structure could impact this. Furthermore, rER becomes disorganized during chromatolysis, which occurs following axonal injury (Gersh and Bodian, 1943). However, the same distribution of ratings, with 2 being most common and 4 being least common, was seen in all groups. This could be a postmortem artifact, or may be the natural state in which rER exists in human SN neurons. Similar findings were seen in mouse spinal motor neurons (Pullen and Humphreys, 2000): the rating equivalent to a 2 in our study was most common. In the mouse spinal motor neurons, however, highly organized rER (a 3 or 4 in our study) was more common than in our study.

4.3 Alterations of myelinated axons

The G-ratio of TR was greater than that of NC by 0.04, indicating that TR have thinner myelin sheaths per size of axon. Although this difference is statistically significant, it is small and may not be functionally significant. A greater G-ratio was seen in adult *rictor* conditional knockout mice (a mouse model of tuberous sclerosis complex), suggesting that the observed 0.04 difference in G-ratios was related to functional differences (West et al., 2015). The G-ratio is lower in humans than mice, so it is possible that more myelin would need to be lost to see functional differences in humans.

In this study, we observed more axons with inclusions in the myelin sheath in SZ. Such inclusions have been noted in prefrontal cortex and caudate nucleus in SZ (Uranova et al., 2001). The effects of such inclusions were not discussed by Uranova and colleagues, but it is possible that disruptions in structure of the myelin sheath could impair action potential propagation, potentially contributing to symptom manifestation.

More axons in TR lacked cytoplasm (empty myelin sheath) and/or contained cellular debris. An empty myelin sheath could reflect profound axonal degeneration at the site where it is observed, or may indicate that the entire axon is gone. Either way, this abnormality is likely

to impact normal connectivity. Empty myelin sheaths have been seen in aged rhesus monkeys, but frequency was not measured (Sandell and Peters, 2003). Studies of blunt contusions in rhesus monkeys and Wallerian degeneration in rats have suggested that these pathologies can occur as a result of damage to the neuron or axon, and that axons may first accumulate cellular debris before eventually degenerating altogether (Bignami et al., 1981; Bresnahan, 1978). In SZ it is unlikely that Wallerian degeneration caused by physical injury is occurring, but axons may be subject to another type of stress resulting in a visually similar response. For instance, it has been shown that excitotoxicity can lead to Wallerian-like axon degeneration in rat optic nerves (Saggu et al., 2010). In fact, the caudate nucleus, a major target of the SN dopamine neurons, has more glutamate in imaging studies (de la Fuente-Sandoval, 2011, 2013) and more glutamate-like terminals in postmortem studies (Roberts et al., 2012). In both instances, these changes were seen in subjects or cases that were treatment resistant.

A number of the axon- and myelin-related pathologies we observed are similar to those seen in an ultrastructural study of natural aging in rats (Xie et al., 2014). Changes common to both studies include vacuolization, condensed cytoplasm, unraveled myelin, and myelin inclusions in the axon. That aging leads to changes in the structure of myelinated axons could explain why many axons were not in perfect condition, but it does not explain differences between groups, since our subjects did not differ significantly in terms of age. However, patients with SZ have shorter lifespans (Laursen et al., 2014), which could indicate accelerated aging, or could be a consequence of lifestyle in SZ.

4.4 Conclusions

Our findings provide support for white matter pathology in schizophrenia. Some of our findings may not be specific to the SN, such as inclusions in the myelin sheath. Despite finding differences between TR and NC, no difference was detected between RESP and TR, which limits our ability to interpret the data as applying to treatment response. Although a previous study (Kolomeets and Uranova, 1999) examined synapses in SN of postmortem schizophrenia using electron microscopy, this study is the first to examine neurons, oligodendrocytes, and myelinated axons in SN in this manner. This is also the first study to investigate treatment response in schizophrenia by studying the SN using electron microscopy. Our findings reveal that much of the ultrastructure of the SN is unchanged in schizophrenia and treatment response, but highlight white matter as a point for future study. Learning more about the underlying structure of the SN as it relates to schizophrenia and treatment response will provide us with a better understanding of the illness and how best to treat it.

Acknowledgments

We thank the staff from the Maryland and Alabama brain collections for the postmortem human brain tissue. We thank the donors and families of the donors for their altruism. This work was funded in part by MH66123 and MH108867 (RCR), and the UAB Honors Neuroscience Research Academy (CKW).

References

Altamura AC, Bassetti R, Cattaneo E, Vismara S. 2005; Some biological correlates of drug resistance in schizophrenia: a multidimensional approach. World J. Biol. Psychiatry. 6(Suppl 2):23–30. [PubMed: 16166020]

American Psychiatric Association. Diagnostic and Statistical Manual of Mental Disorders: DSM-5. American Psychiatric Association; Washington, D.C.: 2013.

Arango C, Breier A, McMahon R, Carpenter WT Jr, Buchanan RW. 2003; The relationship of clozapine and haloperidol treatment response to prefrontal, hippocampal, and caudate brain volumes. Am. J. Psychiatry. 160(8):1421–1427. [PubMed: 12900303]

Bartzokis G, Lu PH, Stewart SB, Oluwadara B, Lucas AJ, Pantages J, Pratt E, Sherin JE, Altshuler LL, Mintz J, Gitlin MJ, Subotnik KL, Nuechterlein KH. 2009; In vivo evidence of differential impact of typical and atypical antipsychotics on intracortical myelin in adults with schizophrenia. Schizophr. Res. 113(2–3):322–331. [PubMed: 19616412]

Beerpoot LJ, Lipska BK, Weinberger DR. 1996; Neurobiology of treatment-resistant schizophrenia: new insights and new models. Eur. Neuropsychopharmacol. 6(Suppl 2):S27–34. [PubMed: 8792118]

Bignami A, Dahl D, Nguyen BT, Crosby CJ. 1981; The fate of axonal debris in Wallerian degeneration of rat optic and sciatic nerves. Electron microscopy and immunofluorescence studies with neurofilament antisera. J. Neuropathol. Exp. Neurol. 40(5):537–550. [PubMed: 7024479]

Bora E, Fornito A, Radua J, Walterfang M, Seal M, Wood SJ, Yücel M, Velakoulis D, Pantelis C. 2011; Neuroanatomical abnormalities in schizophrenia: a multimodal voxelwise meta-analysis and meta-regression analysis. Schizophr. Res. 127(1–3):46–57. [PubMed: 21300524]

Bresnahan JC. 1978; An electron-microscopic analysis of axonal alterations following blunt contusion of the spinal cord of the rhesus monkey (Macaca mulatta). J. Neurol. Sci. 37(1–2):59–82. [PubMed: 99494]

Carlsson A, Lindqvist M. 1963; Effect of chlorpromazine or haloperidol on formation of 3methoxytyramine and normetanephrine in mouse brain. Acta Pharmacol. Toxicol. (Copenh.). 20:140–144. [PubMed: 14060771]

Conley RR, Kelly DL. 2001; Management of treatment resistance in schizophrenia. Biol. Psychiatry. 50(11):898–911. [PubMed: 11743944]

Creese I, Burt DR, Snyder SH. 1977; Dopamine receptor binding enhancement accompanies lesion-induced behavioral supersensitivity. Science. 197(4303):596–598. [PubMed: 877576]

de la Fuente-Sandoval C, Leon-Ortiz P, Azcarraga M, Stephano S, Favila R, Diaz-Galvis L, Alvarado-Alanis P, Ramirez-Bermudez J, Graff-Guerrero A. 2013; Glutamate levels in the associative striatum before and after 4 weeks of antipsychotic treatment in first-episode psychosis: a longitudinal proton magnetic resonance spectroscopy study. JAMA Psychiatry. 70(10):1057–1066. [PubMed: 23966023]

de la Fuente-Sandoval C, Leon-Ortiz P, Favila R, Stephano S, Mamo D, Ramirez-Bermudez J, Graff-Guerrero A. 2011; Higher levels of glutamate in the associative-striatum of subjects with prodromal symptoms of schizophrenia and patients with first-episode psychosis. Neuropsychopharmacology. 36(9):1781–1791. [PubMed: 21508933]

De Peri L, Crescini A, Deste G, Fusar-Poli P, Sacchetti E, Vita A. 2012; Brain structural abnormalities at the onset of schizophrenia and bipolar disorder: a meta-analysis of controlled magnetic resonance imaging studies. Curr. Pharm. Des. 18(4):486–494. [PubMed: 22239579]

Di X, Chan RC, Gong QY. 2009; White matter reduction in patients with schizophrenia as revealed by voxel-based morphometry: an activation likelihood estimation meta-analysis. Prog. Neuropsychopharmacol. Biol. Psychiatry. 33(8):1390–1394. [PubMed: 19744536]

Domesick VB, Stinus L, Paskevich PA. 1983; The cytology of dopaminergic and nondopaminergic neurons in the substantia nigra and ventral tegmental area of the rat: a light- and electron-microscopic study. Neuroscience. 8(4):743–765. [PubMed: 6408498]

Fallon JH, Riley JN, Moore RY. 1978a; Substantia nigra dopamine neurons: separate populations project to neostriatum and allocortex. Neurosci. Lett. 7(2–3):157–162. [PubMed: 19605105]

Fallon JH, Moore RY. 1978b; Catecholamine innervation of the basal forebrain IV: topography of the dopamine projection to the basal forebrain and neostriatum. J. Comp. Neurol. 180(3):545–580. [PubMed: 659674]

Fang F, Zhang H, Zhang Y, Xu H, Huang Q, Adilijiang A, Wang J, Zhang Z, Zhang D, Tan Q, He J, Kong L, Liu Y, Li XM. 2013; Antipsychotics promote the differentiation of oligodendrocyte progenitor cells by regulating oligodendrocyte lineage transcription factors 1 and 2. Life Sci. 93(12–14):429–434. [PubMed: 23973956]

Gaspar P, Stepniewska I, Kaas JH. 1992; Topography and collateralization of the dopaminergic projections to motor and lateral prefrontal cortex in owl monkeys. J. Comp. Neurol. 325(1):1–21. [PubMed: 1362430]

Gersh I, Bodian D. 1943; Some chemical mechanisms in chromatolysis. J. Cell. Comp. Physiol. 21(3): 253–279.

Haijma SV, Van Haren N, Cahn W, Koolschijn PC, Hulshoff Pol HE, Kahn RS. 2013; Brain volumes in schizophrenia: a meta-analysis in over 18 000 subjects. Schizophr. Bull. 39(5):1129–1138. [PubMed: 23042112]

Howes OD, Williams M, Ibrahim K, Leung G, Egerton A, McGuire PK, Turkheimer F. 2013; Midbrain dopamine function in schizophrenia and depression: a post-mortem and positron emission tomographic imaging study. Brain. 136(11):3242–3251. [PubMed: 24097339]

Ichinose H, Ohye T, Fujita K, Pantucek F, Lange K, Riederer P, Nagatsu T. 1994; Quantification of mRNA of tyrosine hydroxylase and aromatic L-amino acid decarboxylase in the substantia nigra in Parkinson's disease and schizophrenia. J. Neural. Transm. Park. Dis. Dement. Sect. 8(1–2):149–158. [PubMed: 7893377]

Kane JM, Honigfeld G, Singer J, Meltzer H. 1988; Clozapine in treatment-resistant schizophrenics. Psychopharmacol. Bull. 24(1):62–67. [PubMed: 3290950]

Kolomeets NS, Uranova NA. 1999; Synaptic contacts in schizophrenia: studies using immunocytochemical identification of dopaminergic neurons. Neurosci. Behav. Physiol. 29(2): 217–221. [PubMed: 10432512]

Kubicki M, McCarley R, Westin CF, Park HJ, Maier S, Kikinis R, Jolesz FA, Shenton ME. 2007; A review of diffusion tensor imaging studies in schizophrenia. J. Psychiatr. Res. 41(1–2):15–30. [PubMed: 16023676]

Kuswanto CN, Teh I, Lee TS, Sim K. 2012; Diffusion tensor imaging findings of white matter changes in first episode schizophrenia: a systematic review. Clin. Psychopharmacol. Neurosci. 10(1):13–24. [PubMed: 23429992]

Laursen TM, Nordentoft M, Mortensen PB. 2014; Excess early mortality in schizophrenia. Annu Rev Clin Psychol. 10:425–48. [PubMed: 24313570]

Lieberman JA, Stroup TS, McEvoy JP, Swartz MS, Rosenheck RA, Perkins DO, Keefe RS, Davis SM, Davis CE, Lebowitz BD, Severe J, Hsiao JK, Clinical Antipsychotic Trials of Intervention Effectiveness (CATIE) Investigators. 2005; Effectiveness of antipsychotic drugs in patients with chronic schizophrenia. New Engl. J. Med. 353(12):1209–1223. [PubMed: 16172203]

Marchese G, Casu MA, Bartholini F, Ruiu S, Saba P, Gessa GL, Pani L. 2002; Sub-chronic treatment with classical but not atypical antipsychotics produces morphological changes in rat nigro-striatal dopaminergic neurons directly related to "early onset" vacuous chewing. Eur. J. Neurosci. 15(7): 1187–1196. [PubMed: 11982629]

McCollum LA, Roberts RC. 2014; Ultrastructural localization of tyrosine hydroxylase in tree shrew nucleus accumbens core and shell. Neuroscience. 271:23–34. [PubMed: 24769226]

McCollum LA, Walker CK, Roche JK, Roberts RC. 2015; Elevated excitatory input to the nucleus accumbens in schizophrenia: a postmortem ultrastructural study. Schizophr. Bull. 41(5):1123–1132. [PubMed: 25817135]

McEvoy JP. 2006; An overview of the Clinical Antipsychotic Trials of Intervention Effectiveness (CATIE) study. CNS Spectrums. 11(7 Suppl 7):4–8.

Meltzer HY. 1997; Treatment-resistant schizophrenia--the role of clozapine. Current Medical Research and Opinion. 14(1):1–20. [PubMed: 9524789]

Mueller HT, Haroutunian V, Davis KL, Meador-Woodruff JH. 2004; Expression of the ionotropic glutamate receptor subunits and NMDA receptor-associated intracellular proteins in the substantia nigra in schizophrenia. Brain Res. Mol. Brain Res. 121:60–69. [PubMed: 14969737]

Niu J, Mei F, Li N, Wang H, Li X, Kong J, Xiao L. 2010; Haloperidol promotes proliferation but inhibits differentiation in rat oligodendrocyte progenitor cell cultures. Biochem. Cell Biol. 88(4): 611–620. [PubMed: 20651832]

Olabi B, Ellison-Wright I, McIntosh AM, Wood SJ, Bullmore E, Lawrie SM. 2011; Are there progressive brain changes in schizophrenia? A meta-analysis of structural magnetic resonance imaging studies. Biol. Psychiatry. 70(1):88–96. [PubMed: 21457946]

Perez-Costas E, Melendez-Ferro M, Rice MW, Conley RR, Roberts RC. 2012; Dopamine pathology in schizophrenia: analysis of total and phosphorylated tyrosine hydroxylase in the substantia nigra. Front. Psychiatry. 3:31. [PubMed: 22509170]

Pullen AH, Humphreys P. 2000; Ultrastructural analysis of spinal motoneurones from mice treated with IgG from ALS patients, healthy individuals, or disease controls. J. Neurol. Sci. 180(1–2):35–45. [PubMed: 11090862]

Rice MW, Smith KL, Roberts RC, Perez-Costas E, Melendez-Ferro M. 2014; Assessment of cytochrome C oxidase dysfunction in the substantia nigra/ventral tegmental area in schizophrenia. PLoS One. 9(6):e100054. [PubMed: 24941246]

Rice MW, Roberts RC, Melendez-Ferro M, Perez-Costas E. 2016; Mapping dopaminergic deficiencies in the substantia nigra/ventral tegmental area in schizophrenia. Brain Struct. Funct. 221(1):185–201. [PubMed: 25269834]

Roberts RC, Force M, Kung L. 2002; Dopaminergic synapses in the matrix of the ventrolateral striatum after chronic haloperidol treatment. Synapse. 45(2):78–85. [PubMed: 12112400]

Roberts RC, Xu L, Roche JK, Kirkpatrick B. 2005; Ultrastructural localization of reelin in the cortex in post-mortem human brain. J Comp Neurol. 482(3):294–308. [PubMed: 15690491]

Roberts RC, Roche JK, Conley RR, Lahti AC. 2009; Dopaminergic synapses in the caudate of subjects with schizophrenia: relationship to treatment response. Synapse. 63:520–530. [PubMed: 19226604]

Roberts, RC, Roche, JK, Somerville, SM, Conley, RR. Ultrastructural distinctions between treatment responders and non-responders in schizophrenia: postmortem studies of the striatum. In: L'Abate, L, editor. Mental Illnesses - Evaluation, Treatments and Implications. InTech. 2012. 261–286.

Saggu SK, Chotaliya HP, Blumbergs PC, Casson RJ. 2010; Wallerian-like axonal degeneration in the optic nerve after excitotoxic retinal insult: an ultrastructural study. BMC Neurosci. 11:97. [PubMed: 20707883]

Samartzis L, Dima D, Fusar-Poli P, Kyriakopoulos M. 2014; White matter alterations in early stages of schizophrenia: a systematic review of diffusion tensor imaging studies. J. Neuroimaging. 24(2): 101–110. [PubMed: 23317110]

Sandell JH, Peters A. 2003; Disrupted myelin and axon loss in the anterior commissure of the aged rhesus monkey. J. Comp. Neurol. 466(1):14–30. [PubMed: 14515238]

Schoonover KE, McCollum LA, Roberts RC. 2017; Protein markers of neurotransmitter synthesis and release in postmortem schizophrenia substantia nigra. Neuropsychopharmacology. 42(2):540–550. [PubMed: 27550734]

Seeman P. 2002; Atypical antipsychotics: mechanism of action. Can. J. Psychiatry. 47(1):27–38. [PubMed: 11873706]

Sheitman BB, Lieberman JA. 1998; The natural history and pathophysiology of treatment resistant schizophrenia. J. Psychiatr. Res. 32(3–4):143–150. [PubMed: 9793867]

Somerville SM, Conley RR, Roberts RC. 2011a; Mitochondria in the striatum of subjects with schizophrenia. World J Biol Psychiatry. 12(1):48–56. [PubMed: 20698738]

Somerville SM, Lahti AC, Conley RR, Roberts RC. 2011b; Mitochondria in the striatum of subjects with schizophrenia: relationship to treatment response. Synapse. 65(3):215–224. [PubMed: 20665724]

Thomas EA. 2006; Molecular profiling of antipsychotic drug function: convergent mechanisms in the pathology and treatment of psychiatric disorders. Mol. Neurobiol. 34(2):109–128. [PubMed: 17220533]

Toru M, Watanabe S, Shibuya H, Nishikawa T, Noda K, Mitsushio H, Ichikawa H, Kurumaji A, Takashinma M, Mataga N, Ogawa A. 1988; Neurotransmitters, receptors, and neuropeptides in post-mortem brains of chronic schizophrenic patients. Acta Psychiatr. Scand. 78:121–37. [PubMed: 2906213]

Uranova N, Orlovskaya D, Vikhreva O, Zimina I, Kolomeets N, Vostrikov V, Rachmanova V. 2001; Electron microscopy of oligodendroglia in severe mental illness. Brain Res. Bull. 55(5):597–610. [PubMed: 11576756]

Uranova NA, Vikhreva OV, Rachmanova VI, Orlovskaya DD. 2011; Ultrastructural alterations of myelinated fibers and oligodendrocytes in the prefrontal cortex in schizophrenia: a postmortem morphometric study. Schizophr. Res. Treatment. 2011:325789. [PubMed: 22937264]

Vikhreva OV, Rakhmanova VI, Orlovskaya DD, Uranova NA. 2016; Ultrastructural alterations of oligodendrocytes in prefrontal white matter in schizophrenia: A post-mortem morphometric study. Schizophr. Res. 177(1–3):28–36. [PubMed: 27156647]

Wang H, Xu H, Niu J, Mei F, Li X, Kong J, Cai W, Xiao L. 2010; Haloperidol activates quiescent oligodendroglia precursor cells in the adult mouse brain. Schizophr. Res. 119(1–3):164–174. [PubMed: 20346631]

Watanabe Y, Tanaka H, Tsukabe A, Kunitomi Y, Nishizawa M, Hashimoto R, Yamamori H, Fujimoto M, Fukunaga M, Tomiyama N. 2014; Neuromelanin magnetic resonance imaging reveals increased dopaminergic neuron activity in the substantia nigra of patients with schizophrenia. PLoS One. 9(8):e104619. [PubMed: 25111500]

West KL, Kelm ND, Carson RP, Does MD. 2015; Quantitative analysis of mouse corpus callosum from electron microscopy images. Data Brief. 5:124–128. [PubMed: 26504893]

White DM, Kraguljac NV, Reid MA, Lahti AC. 2015; Contribution of substantia nigra glutamate to prediction error signals in schizophrenia: a combined magnetic resonance spectroscopy/functional imaging study. NPJ Schizophr. 1:14001. [PubMed: 26878032]

Xiao L, Xu H, Zhang Y, Wei Z, He J, Jiang W, Li X, Dyck LE, Devon RM, Deng Y, Li XM. 2008; Quetiapine facilitates oligodendrocyte development and prevents mice from myelin breakdown and behavioral changes. Mol. Psychiatry. 13(7):697–708. [PubMed: 17684494]

Xie F, Liang P, Fu H, Zhang JC, Chen J. 2014; Effects of normal aging on myelin sheath ultrastructures in the somatic sensorimotor system of rats. Mol. Med. Rep. 10(1):459–466. [PubMed: 24818843]

Yao L, Lui S, Liao Y, Du MY, Hu N, Thomas JA, Gong QY. 2013; White matter deficits in first episode schizophrenia: an activation likelihood estimation meta-analysis. Prog. Neuropsychopharmacol. Biol. Psychiatry. 45:100–106. [PubMed: 23648972]

Yoon JH, Minzenberg MJ, Raouf S, D'Esposito M, Carter CS. 2013; Impaired prefrontal-basal ganglia functional connectivity and substantia nigra hyperactivity in schizophrenia. Biol. Psychiatry. 74(2): 122–129. [PubMed: 23290498]

Yoon JH, Westphal AJ, Minzenberg MJ, Niendam T, Ragland JD, Lesh T, Solomon M, Carter CS. 2014; Task-evoked substantia nigra hyperactivity associated with prefrontal hypofunction, prefrontonigral disconnectivity and nigrostriatal connectivity predicting psychosis severity in medication naive first episode schizophrenia. Schizophr. Res. 159(2–3):521–526. [PubMed: 25266549]

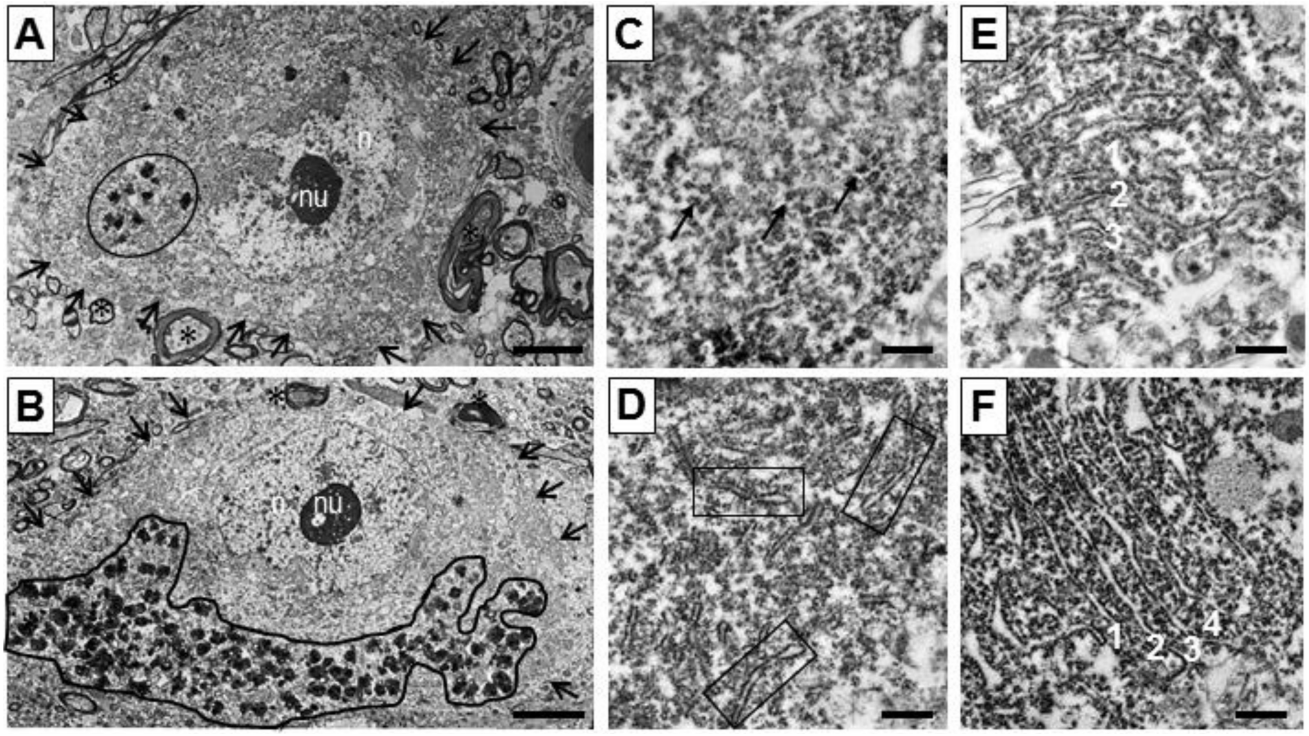

Figure 1.

Neurons and rough endoplasmic reticulum photographed at 5,000× and 25,000×. (A) Neuron from NC. (B) Neuron from SZ. n = nucleus, nu = nucleolus, arrows indicate border of neuron, circle = neuromelanin granules within neuron. (C) Rating = 1, from SZ; arrows = free ribosomes (D) Rating = 2, from NC; boxes = strands of rough ER. (E) Rating = 3, from NC; parallel strands numbered 1–3. (F) Rating = 4, from NC; parallel strands numbered 1–4. Scale bars, (A,B) = 5 μm, (C–F) = 0.5 μm.

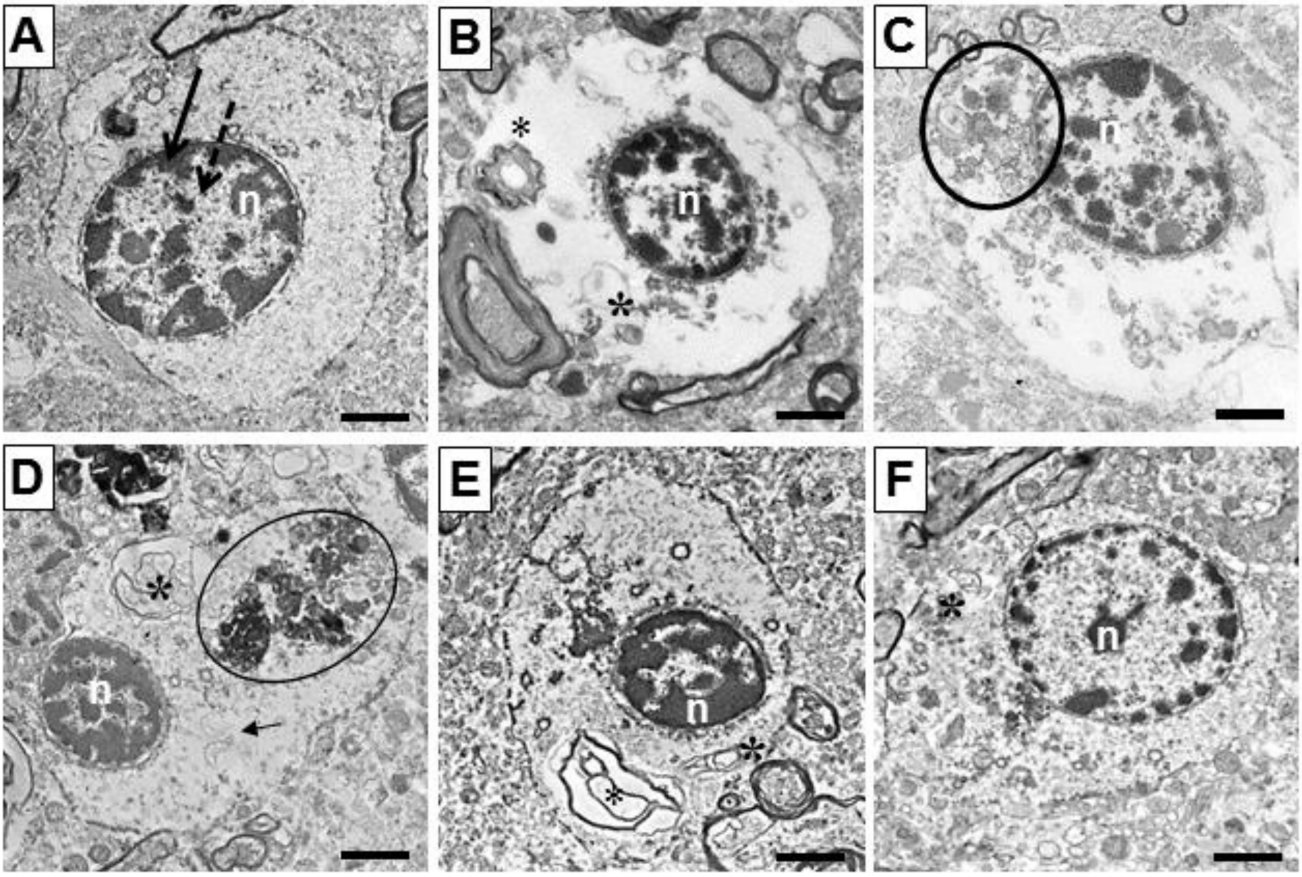

Figure 2.

Oligodendrocytes from NC (A, D, E) and SZ (B, C, F) photographed at 10,000×. (A) Typical oligodendrocyte, with oval nucleus, heterochromatin on nuclear border, defined cellular border, and even density of cytoplasm. (B) Cytoplasmic integrity = 1, vacuous cytoplasm and myelin inclusions present. (C) Cytoplasmic integrity = 2, contains some cytoplasmic contents and amorphous inclusions. (D) Cytoplasmic integrity = 3, more intact cytoplasm but amorphous, myelin, and filamentous cellular inclusions. (E) Cytoplasmic integrity = 4, mostly intact cytoplasm with myelin inclusions present. (F) Cytoplasmic integrity = 5, totally intact cytoplasm, with one myelin inclusion present. n = nucleus, circle = amorphous inclusion, * = myelin inclusion, arrow = filamentous cellular inclusion. Scale bars= 2 μm.

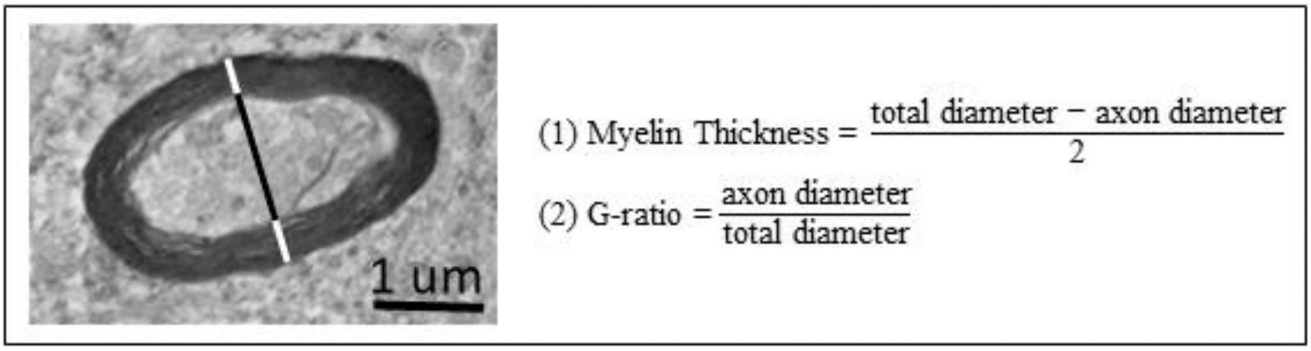

Figure 3.

A myelinated axon is shown along with the formula to calculate myelin thickness and G ratio. Black line = axon diameter. Black + white lines = total diameter.

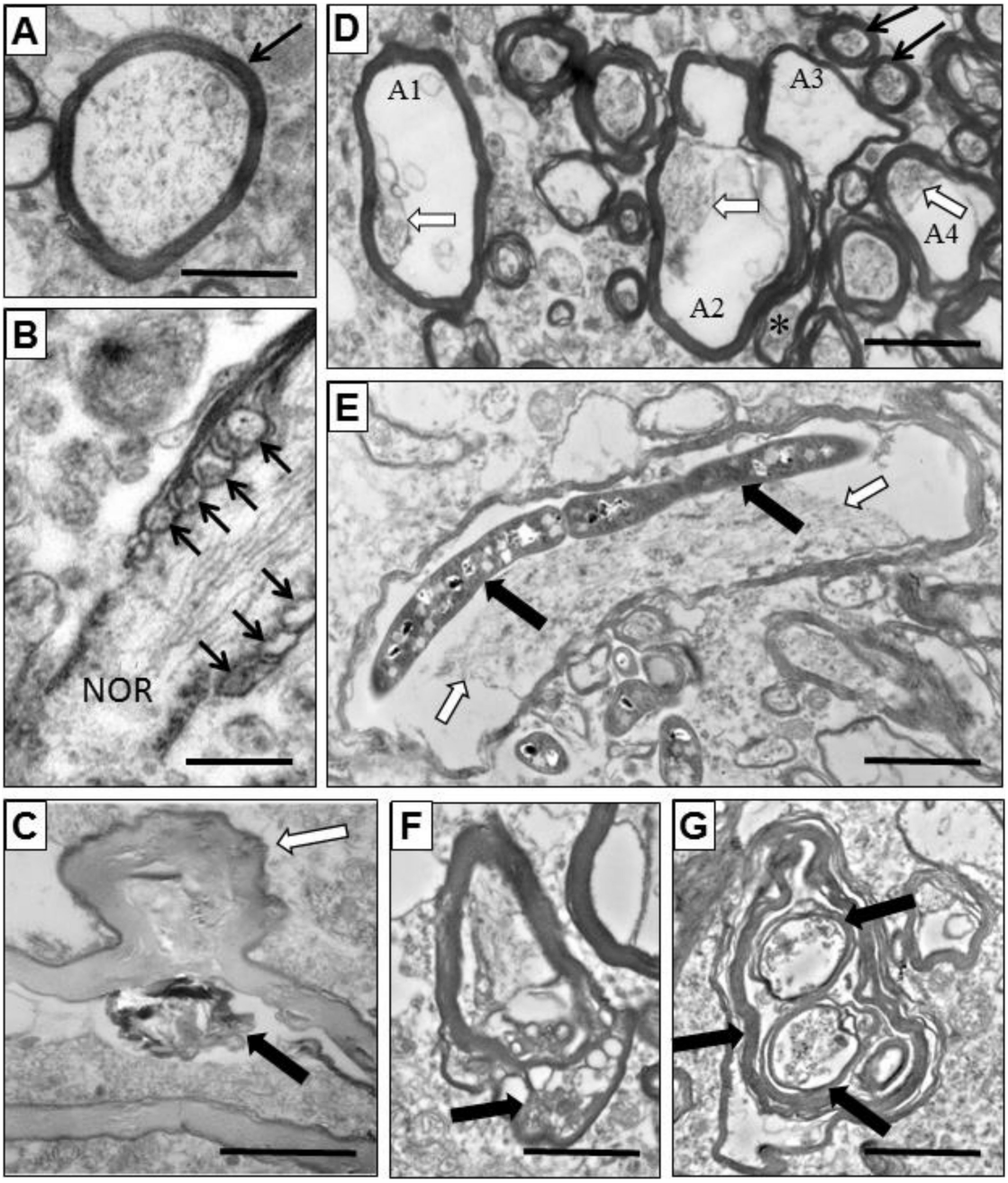

Figure 4.

Myelinated axons from NC (A) and SZ (B–G) subjects. (A) Axon with normal contents and myelin sheath (black arrow). (B) Myelinated axon unfurling (arrows) to form a node of Ranvier (NOR). (C) Axon with hypodense myelin sheath, cellular debris (solid arrow), and a protrusion of the myelin sheathe (black and white arrow). (D) Normal (black arrows) and damaged axons (A1–A4). Axon 1 has a normal myelin sheath, but less than 10% of cytoplasm remains (arrow). Axon 2 and 4 have normal myelin, but greatly diminished and displaced cytoplasm (arrows). Axon 3 has no axonal contents, a thin myelin sheath and a redundant myelin tail (*). (E) Axon with displaced cytoplasm (black and white arrows) and

a large inclusion (black arrows). (F) Axon with inclusions within the myelin sheath (arrow). (G) Abnormal axon with several discrete myelin sheathes (thick black arrows) within. Scale bars (B) =0.5 μm, (A,CG) = 2 μm.

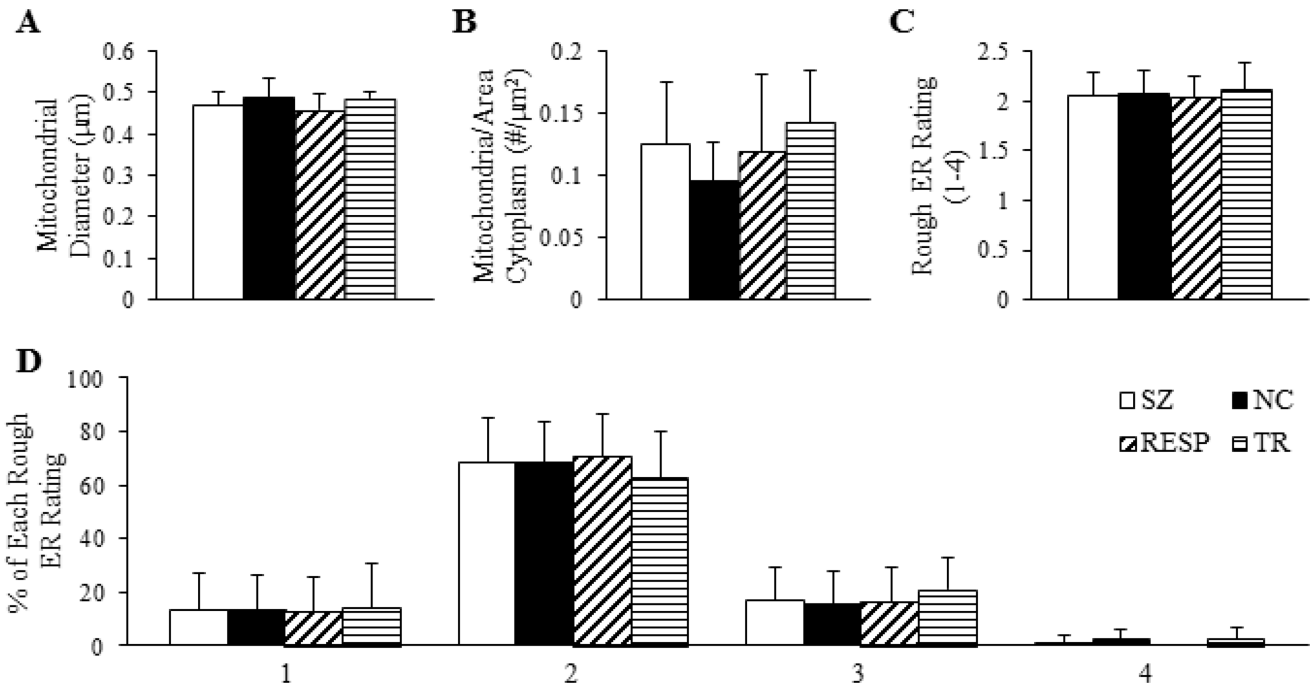

Figure 5.

Measurements of mitochondria and rough ER in neurons. (A) Diameter of mitochondria in the soma. (B) Density of mitochondria in the cytoplasm, measured as the number of mitochondria per square micron of cytoplasm. (C) Average rating of organization (1–4) of rough ER. (D) Percentage of each rough ER organization rating.

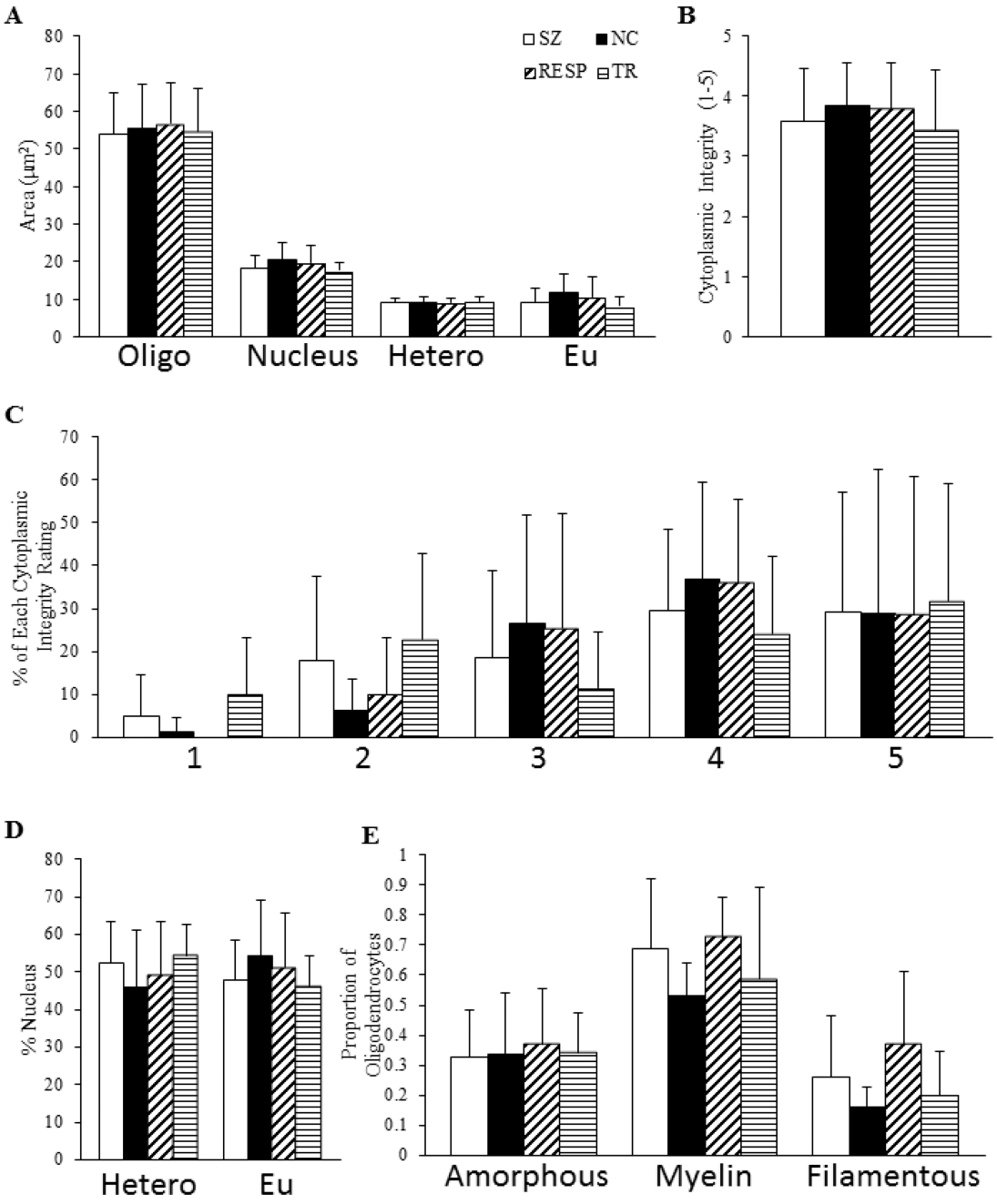

Figure 6.

Qualitative and quantitative oligodendrocyte measurements. (A) Average area of oligodendrocyte, nucleus, heterochromatin, and euchromatin. (B) Average rating of cytoplasmic integrity. (C) Percentage of oligodendrocytes with each cytoplasmic integrity rating. (D) Percent of the nucleus containing heterochromatin and euchromatin. (E) Proportion of oligodendrocytes containing amorphous, myelin, or filamentous cellular inclusions.

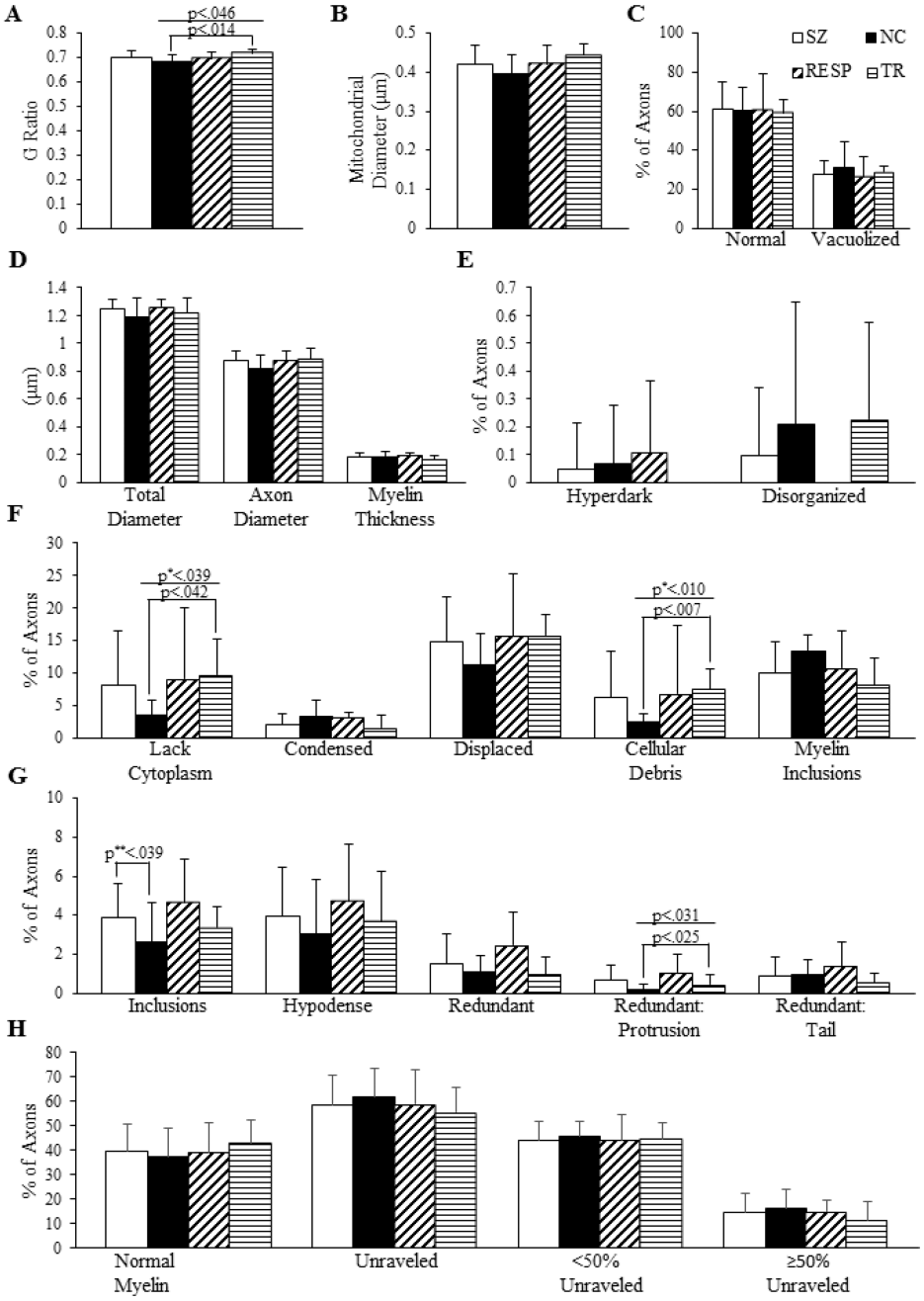

Figure 7.

Qualitative and quantitative measurements of myelinated axons. (A) G-ratio. (B) Diameter of mitochondria in axons. (C, E, F) Percentage of axons with listed characteristics. (D) Total and axon diameters and myelin thickness. (G, H) Percentage of axons with listed characteristics.

Table 1

Case Demographics

	#	Age	pH	PMI (h)	Age of Onset	Duration	APD		Race	Sex
NC	9	43.9±14.3	6.9±0.3	5.9±1.5					4AA, 5C	4F, 5M
SZ	14	48.3±11.4	6.9±0.3	6.1±2.3	22.3±5.6	24.8±10.5	7A, 4T		7AA, 7C	5F, 9M
t-test		0.42	0.85	0.84				χ^2	0.80	0.68
TR	6	40.2±8.4	6.8±0.2	7.0±2.8	19.8±4.7	24.3±8.9	4A, 0T		2AA, 4C	3F, 3M
RESP	6	51.3±8.8	7.0±0.3	5.2±1.9	24.4±5.8	25.2±12.6	2A, 4T		3AA, 3C	2F, 4M
ANOVA/t-test		0.25	0.82	0.32	0.24	0.90	**.007**	χ^2	0.56	0.56

Mean±standard deviation, NC = normal control, SZ = schizophrenia, RESP = treatment responder, TR = treatment resistant, AA = African American, C = Caucasian, F = female, M = male, PMI = postmortem interval.